Leader-Follower Cooperative Manipulation Under Spatio-Temporal Constraints

Mayank Sewlia, Christos K. Verginis, and Dimos V. Dimarogonas

***Abstract*— In this work, we develop a control algorithm for mobile manipulators manipulating an object within a leader-follower framework. Unlike existing literature, we avoid the knowledge of the object's dynamics, and only the leader is aware of the tasks to be executed by the object. The followers are primarily tasked to lift the object and maintain a desired posture while the leader manipulates the object despite its unknown dynamic parameters. We employ a stiffness-based controller for the followers, allowing set-point stabilisation with permissible flexibility and a high-gain prescribed performance controller for the leader to facilitate manipulation from the object's equilibrium state. We present simulation results with two followers and one leader KUKA youbots to validate our proposed framework.**

I. Introduction

The cooperative manipulation problem involves manipulating a payload when a single agent is unable to carry the object alone. Such an approach offers advantages but also introduces certain challenges, including coordinating motion among robots, evenly distributing the load, performing decentralised planning, and translating high-level tasks for the object into low-level tasks for individual joint angles. The problem becomes more structured when there is a hierarchy among the robots, allowing some agents to assume greater leadership roles in the tasks. Such a leader-follower framework emerges naturally in various scenarios of cooperative manipulation. For instance, a leader agent might (i) possess powerful actuators enabling it to lift heavier payloads, (ii) be equipped with a greater number of degrees of freedom, (iii) have comprehensive knowledge of the environment and the locations of obstacles, or (iv) have access to the desired tasks — which is the focus of this study.

The premise of this work is thus to explore the cooperative manipulation of an object when only a subset of the agents are aware of the desired tasks associated with the object. For instance, a task could involve picking and placing an object within specific timing constraints. We refer to these tasks as spatio-temporal tasks, which impose both spatial and temporal requirements. By allocating the task knowledge to a specific subset of agents, we enable the remaining agents to dedicate themselves to other secondary but important tasks, such as helping to carry the payload. In our approach, the follower agents are responsible for lifting the object and compensating for its gravity, whereas the leader agent is charged with manipulating the object according to specified requirements. Nevertheless, we proceed under the assumption that there is no knowledge of the dynamical terms of the robots and the object, and we abstain from using force measurements to identify any external forces exerted by the leader agents. The control challenge is divided into designing a controller for the follower agents to compensate for the object's gravitational forces and for the leader agent to guide the object along a desired trajectory. We consider mobile manipulators as they allow for larger workspace accessibility and enable the utilisation of redundant degrees of freedom to perform secondary tasks for the mobile bases.

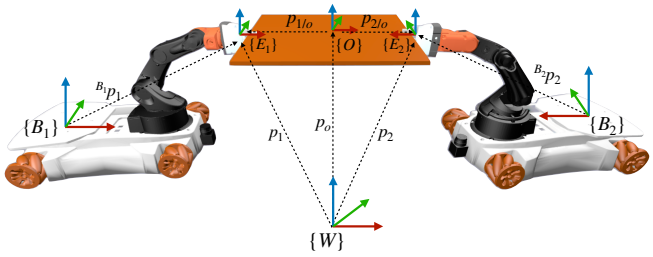

Fig. 1: Two mobile manipulators grasping an object

In this regard, our approach unfolds as follows: We first design a decentralised stiffness controller for each follower agent to compensate for the object's gravitational forces. This controller incorporates adaptive gravity compensation for the object since its mass is unknown to the agents. Additionally, a decentralized controller is not associated with real-time problems, such as channel overload or latency, which can arise over a communication network. Consequently, it enables the follower-object agents system to behave like a mass-spring-damper system, which a leader agent can then manipulate. To this end, we develop a prescribed performance control (PPC) for the leader agent, which is tasked with enforcing spatio-temporal constraints on the object. The contributions of this work are stated as follows: (i) We design a novel controller enabling followers to cooperatively manipulate an object, along with a mechanism for the leader to perform trajectory tracking; (ii) We introduce a robust framework for the leader-follower configuration that facilitates the transportation of the object, implemented without requiring full knowledge of the dynamical properties of the system; and (iii) We finally present simulation results to validate the proposed framework.

*This work was supported by the ERC CoG LEAFHOUND, the Swedish Research Council (VR), the Knut och Alice Wallenberg Foundation (KAW) and the H2020 European Project CANOPIES.

M. Sewlia and D. V. Dimarogonas are with Division of Decision and Control, School of EECS, KTH Royal Institute of Technology, 100 44 Stockholm, Sweden. {sewlia, dimos}@kth.se

Christos K. Verginis is with Division of Signals and Systems, Department of Electrical Engineering, Uppsala University, Uppsala, Sweden. christos.verginis@angstrom.uu.se

The rest of the paper is organized as follows: Section II presents the related literature, followed by notations in Section III. The problem formulation, along with system dynamics and control design, is presented in Section IV. Section V presents the main results, and Section VI showcases simulation results to validate the proposed framework. Finally, the conclusion is provided in Section VII.

II. Related Work

We review the literature in three categories that contribute to our discussions later: adaptive control with gravity compensation, compliant control of cooperative manipulators, and the enforcement of spatio-temporal constraints within compliant manipulators.

A foundational approach in robotics has been the parameterisation of unknown system dynamics coupled with adaptive control. Studies spanning from the early 1980s, such as [1], [2], and [3], to more recent contributions like [4], illustrate the evolution of adaptive control for robotics manipulators. However, parameterising the entire dynamics does come with the cost of increased computational demands and poor performance. An alternative is to only parameterise the gravity terms and use a Proportional-Derivative (PD) controller, such as [5] presented for a single manipulator setting. Works such as [6] and [7] study compliant control for manipulators both in a single-agent and a multi-agent setting. However, such methods require and make use of the knowledge of the centrifugal and Coriolis terms of the system. Impedance control of manipulators, studied in [8] and [9], shapes the impedance behaviour of a system, often involving either the acceleration measurements or the measurements of the external forces. This could be circumvented by designing a force estimator [10] or treating the forces as disturbances and designing a disturbance observer [11]–[13], still requiring, however, the knowledge of the dynamical terms.

Closely related problems were studied in [14], [15] and [16]. In [14], the authors used an inverse dynamics controller to design an impedance control scheme along with an estimation law to estimate the leader's intention. In [15], an impedance controller and a wrench estimator are designed to capture the human's intention in transporting the object. The assumption of knowing the inertial and Coriolis terms of agents and object is made in both the above works such that the controller is able to shape the dynamics in a satisfactory manner. In [16], the authors study the cooperative manipulation problem using adaptive control, where all the robots work cooperatively to track the reference trajectory. The dynamics of the system are parameterised, and redundancy resolution is discussed.

In our previous work, [17], we explored cooperative manipulation in a homogenous group of agents where every agent knew the desired satisfactory tasks. Unlike the literature discussed above, here, we work with mobile manipulators, restrict the knowledge of tasks to only a subset of agents and are able to enforce transient constraints without the knowledge of the dynamical terms of the system.

III. Notations

The set of real numbers are denoted by $\mathbb{R}$ and the set of natural numbers by $\mathbb{N}$. With $n, m \in \mathbb{N}$, $\mathbb{R}^n$ is the set of n-coordinate real-valued vectors, $\mathbb{R}^{n\times m}$ represent matrices of size $n \times m$ with real numbers and $\mathbb{R}_+$ is the set of positive real number. By $\mathbf{0}^{n\times m}$ we denote a matrix of size $n \times m$ with all 0 elements. For $a, b \in \mathbb{R}^3$, $S(a)$ denotes a skew-symmetric matrix defined as $S(a)b = a \times b$, where $\times$ is the vector-cross product operator. We denote by $\mathbb{T}^3$ the 3D torus.

IV. Problem Statement

In this section, we begin by presenting the system dynamics followed by the proposed problem statement. The system dynamics encompass the dynamics of the follower agents, the leader agents, the object, the coupled follower-object dynamics, and the coupled leader-follower-object dynamics.

A. System Dynamics

Let the total number of agents be $N = N_f + N_l$ where N_f represents the number of follower agents, and N_l represents the number of leader agents. Each agent consists of $n_i \geq 6$ joint-space variables $q_i \in \mathbb{R}^{n_i}$. The pose of the ith end-effector, $x_i = [p_i^\top, \eta_i^\top]^\top$ is the operational space pose, and $v_i = [\dot{p}_i^\top, \omega_i^\top]^\top$ is the operational space velocity. The pose comprises the position $p_i \in \mathbb{R}^3$ and the Euler angles $\eta_i \in \mathbb{T}^3$, while the velocity v_i consists of the rate of change of position $\dot{p}_i \in \mathbb{R}^3$ and the angular velocity $\omega_i \in \mathbb{R}^3$. The differential kinematics $v_i = J_i(q_i)\dot{q}_i$ relate the joint angle rate to the operational space velocity with the kinematic Jacobian $J_i(q_i) : \mathbb{R}^{n_i} \to \mathbb{R}^{6\times n_i}$.

The operational space agent dynamics is given by [18],

$$M_i(q_i)\dot{v}_i + C_i(q_i, \dot{q}_i)v_i + g_i(q_i) = u_i - h_i \tag{1}$$

where $M_i : \mathbb{R}^{n_i} \to \mathbb{R}^{6\times 6}$ is the positive-definite inertia matrix, $C_i : \mathbb{R}^{2n_i} \to \mathbb{R}^{6\times 6}$ is the Coriolis matrix, $g_i : \mathbb{R}^{n_i} \to \mathbb{R}^6$ is the gravity vector, $u_i \in \mathbb{R}^6$ is the input wrench at the end-effector and $h_i \in \mathbb{R}^6$ is the generalised force exerted on the environment by the end-effector. To convert the input wrench at the end-effector into the applied torques for each actuator of the robot, we utilize the following relationship: $\tau_i = J_i(q_i)^\top u_i$where $\tau_i \in \mathbb{R}^{n_i}$. The agent dynamics can be written in vector form as,

$$M_f(q)\dot{v}_f + C(q, \dot{q})v_f + g_f(q) = u_f - h_f \tag{2}$$

for the follower agents and

$$M_l(q)\dot{v}_l + C(q, \dot{q})v_l + g_l(q) = u_l - h_l \tag{3}$$

for the leader agents. Here $M_{\{f,l\}} = \text{diag}([M_i]) \in \mathbb{R}^{6N_{\{f,l\}}\times 6N_{\{f,l\}}}$, $C_{\{f,l\}} = \text{diag}([C_i]) \in \mathbb{R}^{6N_{\{f,l\}}\times 6N_{\{f,l\}}}$, $g_{\{f,l\}} = [g_1^\top, \ldots, g_{N_{\{f,l\}}}^\top]^\top \in \mathbb{R}^{6N_{\{f,l\}}}$, $u_{\{f,l\}} = [u_1^\top, \ldots, u_{N_{\{f,l\}}}^\top]^\top \in \mathbb{R}^{6N_{\{f,l\}}}$, and $h_{\{f,l\}} = [h_1^\top, \ldots, h_{N_{\{f,l\}}}^\top]^\top \in \mathbb{R}^{6N_{\{f,l\}}}$.

The pose and velocity of the object's centre of mass are denoted by $x_o = [p_o^\top, \eta_o^\top]^\top$ and $v_o = [\dot{p}_o^\top, \omega_o^\top]^\top$, respectively. The velocity is related to the rate of change of position by $v_o = J_{o_r}(x_o)\dot{x}_o$ where $J_{o_r} : \mathbb{R}^3 \times \mathbb{T}^3 \to \mathbb{R}^{6\times 6}$

is the object representation Jacobian. The object's dynamics are,

$$M_o(x_o)\dot{v}_o + C_o(x_o, v_o)v_o + g_o = h_o \tag{4}$$

where $M_o : \mathbb{R}^3 \times \mathbb{T}^3 \to \mathbb{R}^{6\times6}$ is the positive-definite inertia matrix, $C_o : \mathbb{R}^3 \times \mathbb{T}^3 \times \mathbb{R}^6 \to \mathbb{R}^{6\times6}$ is the Coriolos matrix, $g_o : \mathbb{R}^3 \times \mathbb{T}^3 \to \mathbb{R}^6$ is the gravity vector and $h_o \in \mathbb{R}^6$ is the force acting on the objects centre of mass.

We consider rigid grasps in this work, which gives rise to the relationship

$$p_i = p_o + p_{i/o}, \quad \eta_i = \eta_o + \eta_{i/o} \tag{5}$$

where $p_{i/o}$ and $\eta_{i/o}$ are the constant position and orientation offsets among the ith end-effector and the object's center of mass. Without the leader, the coupled follower-object dynamics is given by balancing the forces the followers exert on the object at grasping points to the forces experienced by the object's centre of mass, i.e., $h_o = G_f^\top h_f$ where $G_f : \mathbb{R}^{n_i N_f} \to \mathbb{R}^{6N_f\times6}$ is the grasp matrix. The grasp matrix $G_f = [J_{o_1}^\top(q_1), \ldots, J_{o_{n_f}}^\top(q_{n_f})]^\top$ is composed of the object to the ith agent Jacobian $J_{o_i}(q_i) : \mathbb{R}^{n_i} \to \mathbb{R}^{6\times6}$ given by,

$$J_{o_i}(q_i) = \begin{bmatrix} I_3 & S(-p_{i/o}(q_i)) \\ 0_{3\times3} & I_3 \end{bmatrix}. \tag{6}$$

The resulting coupled follower-object dynamics are,

$$\tilde{M}_f(q)\dot{v}_o + \tilde{C}_f(q,\dot{q})v_o + \tilde{g}_f(q,\dot{q}) = G_f^\top(q)u_f \tag{7}$$

where $\tilde{M}_f(q) = M_o(q) + G_f^\top(q)M_f(q)G_f(q)$, $\tilde{C}_f(q,\dot{q}) = C_o(q,\dot{q}) + G_f^\top(q)M_f(q)\dot{G}_f(q) + G_f^\top(q)C_f(q,\dot{q})G_f(q)$ and $\tilde{g}_f(q,\dot{q}) = g_o(q) + G_f^\top(q)g_f(q)$.

Finally, the coupled leader-follower-object dynamics is obtained by balancing the forces exerted both by the follower agents and the leader agents on the object, i.e., $h_o = G_f u_f + G_l u_l$, resulting in,

$$\tilde{M}(q)\dot{v}_o + \tilde{C}(q,\dot{q})v_o + \tilde{g}(q,\dot{q}) = G_f^\top(q)u_f + G_l^\top(q)u_l \tag{8}$$

where, $\tilde{M} = \tilde{M}_f + G_l M_l G_l^\top$, $\tilde{C} = \tilde{C}_f + G_l M_l \dot{G}_l^\top + G_l C_l G_l^\top$ and $\tilde{g} = \tilde{g}_f + G_l^\top g_l$.

B. Signal Temporal Logic (STL)

We consider that the spatio-temporal task assigned to the multi-robot system is expressed via signal temporal logic (STL) specifications[1]. STL is a predicate-based logic that allows for continuous-time spatial and temporal constraints [19]. Consider the following fragment of the STL syntax,

$$\psi ::= \top \mid \mu \tag{9a}$$

$$\phi ::= \psi \mid \mathcal{G}_{[a,b]}\psi \mid \mathcal{F}_{[a,b]}\psi \mid \phi_1 \wedge \phi_2 \tag{9b}$$

where ϕ_1, ϕ_2 are STL formulas of the form ϕ, $b \geq a \geq 0$ and μ is a predicate of the form $\mu : \mathbb{R}^n \times \mathbb{R}_{\geq0} \to \mathbb{B}$ defined via a predicate function $p : \mathbb{R}^n \times \mathbb{R}_{\geq0} \to \mathbb{R}$ as

$$\mu = \begin{cases} \top & p(\mathbf{x}, t) \geq 0 \\ \bot & p(\mathbf{x}, t) < 0 \end{cases}. \tag{10}$$

[1]the proposed framework can accommodate other types of task models.

The satisfaction relation of a continuous-time signal $\mathbf{x} : \mathbb{R}_{\geq0} \to \mathbb{R}^n$ represented by $(\mathbf{x}, t) \models \phi$ indicates that signal $\mathbf{x}$ satisfies ϕ at time t and is defined recursively as follows:

$$\begin{aligned}
&(\mathbf{x}, t) \models \mu && \Leftrightarrow p(\mathbf{x}, t) \geq 0 \\
&(\mathbf{x}, t) \models \phi_1 \wedge \phi_2 && \Leftrightarrow (\mathbf{x}, t) \models \phi_1 \wedge (\mathbf{x}, t) \models \phi_2 \\
&(\mathbf{x}, t) \models \mathcal{G}_{[a,b]}\psi && \Leftrightarrow \forall t_1 \in [t+a, t+b] s.t. (\mathbf{x}, t_1) \models \psi \\
&(\mathbf{x}, t) \models \mathcal{F}_{[a,b]}\psi && \Leftrightarrow \exists t_1 \in [t+a, t+b] s.t. (\mathbf{x}, t_1) \models \psi
\end{aligned}$$

STL can express constraints such as 'Let the signal $\mathbf{x}$ be $\epsilon-$close to point A in the entire time interval $[5, 10]$s and let the signal $\mathbf{x}$ be $\epsilon-$close to point B sometime in the time interval $[10, 15]$s', with the following formula,

$$\phi = \mathcal{G}_{[5,10]}\Big(\|\mathbf{x} - A\| \leq \epsilon\Big) \wedge \mathcal{F}_{[10,15]}\Big(\|\mathbf{x} - B\| \leq \epsilon\Big)$$

for some $\epsilon > 0$.

The setup includes having both follower and leader agents as mobile manipulators, consisting of both a mobile base and a manipulator arm. This arrangement provides us with redundant degrees of freedom, allowing for the prescription of additional tasks in the redundant directions. The problem then is to design u_f and u_l, such that the object satisfies a user-defined STL formula. More formally,

Problem 1: Consider a system comprising $N = N_f + N_l$ agents and a spatio-temporal tasks encoded via an STL formula ϕ. Design a decentralised stiffness controller, $u_f \in \mathbb{R}^{6N_f}$, enabling the follower agents to lift the rigidly grasped object. Concurrently, design a controller $u_l \in \mathbb{R}^{6N_l}$ for the leader agents, ensuring that it can effectively manipulate the object to satisfy ϕ.

V. Main Results

The solution approach we adopt is outlined as follows:

(A) Design an adaptive update law for the followers to compensate for the object's gravity vector g_o.

(B) Design u_f for the follower agents such that the dynamics (7) take the following form,

$$\tilde{M}_f\dot{v}_o + (\tilde{C}_f + K_v)v_o - J_{o_r}^{-1}K_x\Delta x_e = 0 \tag{11}$$

where K_x and K_v are the desired stiffness and damping matrices, respectively, and Δx_e denotes a position error to be specified later. This allows the follower-object system to behave like a mass-spring-damper system, allowing us to exert forces on a virtual spring with the desired stiffness and damping properties.

(C) Develop the implementation of u_f to map to joint torques τ_f, considering the redundant degrees of freedom inherent in the mobile manipulator.

(D) Design a suitable controller u_l for the leader to impose the desired spatio-temporal tasks on the object.

A. Adaptive Gravity Compensation

The gravity vector g_o of the object can be parameterised as [2],

$$g_o = Y_o\gamma_o \tag{12}$$

where Y_o is a known regressor matrix and γ_o is the unknown parameter vector. Define the adaptive update law as

$$\dot{\hat{\gamma}}_o = -\Gamma Y_o v_o \tag{13}$$

where Γ is a diagonal matrix composed of positive parameters.

B. Follower-Only Controller Design

We are now ready to design the controller u_f for the follower agents with the goal to shape the dynamics (7) into (11) in order to stabilise the object's position x_o around a time-varying desired pose x_{o_d}, with the error represented by $\Delta x_e = x_{o_d} - x_o$. We select x_{o_d}as an exponential moving average of x_o, governed by the stable dynamics $\tau \dot{x}_{o_d} + x_{o_d} = x_o$ where τ is a positive time constant. This formulation of the error will allow the follower-object system to function akin to a mass-spring-damper system around the equilibrium point x_{o_d}. By establishing such a moving average, we aim to ensure that the object stabilises around this point in the absence of external forces applied by the leader agent. Such a low pass filter provides robustness and a degree of compliance to external disturbances. We now design the stiffness-based adaptive controller for the followers as follows:

$$u_f = g_f + G_f^+(Y_o\hat{\gamma}_o + J_{o_r}^{-1}K_x\Delta x_e - K_v v_o) \tag{14}$$

where $G_f^+ = [J_{o_1}^{-1}(q_1), \ldots, J_{o_N}^{-1}(q_{N_f})] \in \mathbb{R}^{6N_f \times 6}$.

Note that we employ a stiffness-based controller rather than an impedance-based controller. The rationale for this choice stems from the fact that impedance control requires shaping the desired inertia matrix, a task generally avoided due to the complexity of designing and calculating the inertia matrix. Furthermore, impedance control requires measuring the object's acceleration, which tends to be a highly noisy signal or requires measuring external wrenches [6]. Now, we are ready to prove the stability of the follower-object system. This proof is necessary because, when the leader is not manipulating the object, we require the follower-object system to still stabilise around the pose where the leader last released the object.

Theorem 1: Consider N_f followers rigidly grasping an object with the coupled dynamics (7). Then, under the adaptive control law (14) and the estimation update law (13), the object pose x_o is asymptotically stabilised around the pose x_{o_d}.

Proof: We first construct the following positive-definite Lyapunov function candidate

$$V = \frac{1}{2}v_o^\top \tilde{M}_f v_o + \frac{1}{2}\tilde{\gamma}_o\Gamma^{-1}\tilde{\gamma}_o + \frac{1}{2}\Delta x_e^\top K_x \Delta x_e \tag{15}$$

where $\tilde{\gamma}_o = \gamma_o - \hat{\gamma}_o$ is the estimation error vector. Taking the time derivative of the above candidate function,

$$\begin{aligned}\dot{V} &= v_o^\top \tilde{M}_f \dot{v}_o + \frac{1}{2}v_o^\top \dot{\tilde{M}}_f v_o + \tilde{\gamma}_o\Gamma^{-1}\dot{\tilde{\gamma}}_o + \Delta x_e^\top K_x \Delta \dot{x}_e \\ &= v_o^\top(G_f u_f - Y_o\gamma_o - G_f g_f) + \frac{1}{2}v_o^\top(\dot{\tilde{M}}_f - 2\tilde{C}_f)v_o + \\ &\tilde{\gamma}_o\Gamma^{-1}\dot{\tilde{\gamma}}_o + \Delta x_e^\top K_x \Delta \dot{x}_e\end{aligned}$$

Now note that, $\dot{\tilde{\gamma}}_o = \dot{\hat{\gamma}}_o$, $\Delta\dot{x}_e = \dot{x}_{o_d} - \dot{x}_o = -\frac{\Delta x_e}{\tau} - J_{o_r}^{-1}v_o$, and, $\dot{\tilde{M}}_f - 2\tilde{C}_f$ is skew-symmetric [3]. Hence,

$$\begin{aligned}\dot{V} =& v_o^\top(G_f u_f - Y_o\gamma_o - G_f g_f - J_{o_r}^{-1}K_x\Delta x_e) + \\ &\tilde{\gamma}_o\Gamma^{-1}\dot{\hat{\gamma}}_o - \Delta x_e^\top \frac{K_x}{\tau}\Delta x_e\end{aligned}$$

Furthermore, using (14) and (13) in the above equation, we obtain the bound as follows,

$$\begin{aligned}\dot{V} &= v_o^\top(Y_o\hat{\gamma}_o - Y_o\gamma_o) + \tilde{\gamma}_o^\top Y_o v_o - v_o^\top K_v v_o - \Delta x_e^\top \frac{K_x}{\tau}\Delta x_e \\ &= -v_o^\top K_v v_o - \Delta x_e^\top \frac{K_x}{\tau}\Delta x_e \leq 0.\end{aligned}$$

The above function is negative semi-definite and vanishes if and only if $v_o = 0$ and $\Delta x_e = 0$. By applying the Lasalle invariance principle [20], the theorem is proved. ∎

The controller (14) is decentralised due to the grasp matrix term G_f^+, and follower each agent i implements its corresponding

$$u_{f_i} = g_{f_i} + J_{o_i}^{-1}(Y_o\hat{\gamma}_o + J_{o_r}^{-1}K_x\Delta x_e - K_v v_o).$$

Also, observe that we can choose small gains for K_x and K_v as we do not enforce strict trajectory tracking requirements with respect to x_{o_d}. Other approaches, such as solely performing gravity compensation on the object, could result in the object moving indefinitely once the leader releases it. Alternatively, defining a static setpoint might force the object to return to this fixed point after manipulation, which undermines the task being performed. A more natural choice is to allow the object to stabilize around the point where the leader last released it; this rationale motivates the design of the desired position as an exponential moving average. By doing this, we also enforce a certain degree of compliance in the system. Additionally, in the simulations, we observed that the adaptive estimate of the object's mass, $\hat{\gamma}_o = \hat{m}_o$, actually converges to $1/N_f$-th of the original estimate. This makes intuitive sense as we expect all the N_f followers to share the load equally; proving this relationship is part of the future work. Next, we will explore how to implement such a controller on mobile manipulators and also how to exploit the redundant degrees of freedom natural to such robots.

C. Implementation of Follower Controller

Here, we demonstrate how to distribute the input wrench into torques for the mobile base and the manipulator. Define ${}^{B_i}p_i \in \mathbb{R}^6$ (see Figure 1) as the pose vector of the end-effector $\{E_i\}$ in the frame of the mobile base $\{B_i\}$. Partition the joint-space states into those pertaining to the mobile base and those belonging to the manipulator. Denote $n_i = n_i^b + n_i^m$, where n_i^b represents the degrees of freedom of the mobile base, and n_i^m represents the degrees of freedom of the manipulator. The torques $\tau_i = [(\tau_i^b)^\top, (\tau_i^m)^\top]^\top$ and the Jacobian $J_i = [J_i^b, J_i^m]$ are partitioned into components associated with the base and the manipulator, respectively. To utilize the redundant degrees of freedom provided by the mobile manipulator, we employ the null-space projection of the Jacobian [21]. Through the null space, we facilitate

the motion of the base without affecting the motion of the end-effector. The intuition is to enable the base to follow the object by detecting changes only in the ${}^{B_i}p_i$ vector. By implementing such a strategy, the entire follower-object structure would detect changes in the position of the end-effector and compensate individually by generating motions in the null space. The implementation we propose is,

$$\tau_i = J_i^\top u_i + (I - J_i^+ J_i) \begin{bmatrix} \tau_{b_i} \\ \mathbf{0}^{m_i^m \times 1} \end{bmatrix}$$

where J_i^+ is the pseudo-inverse and $\tau_{b_i} \in \mathbb{R}^{n_i^b}$ is the mobile base controller given by,

$$\tau_{b_i} = -J_i^b K_{b_x} ({}^{B_i}p_i^d - {}^{B_i}p_i).$$

Here, K_{b_x} is a positive-definite gain matrix and ${}^{B_i}p_i^d$ represents the desired pose of the end-effector. In this work, we have chosen this vector to correspond to the pose at the initial grasp. This approach ensures that the base tracks the movement of the object in response to any external forces applied to the end-effector, allowing for the coordinated movement of the entire follower-object assembly through this localized implementation of the base controller.

D. Leader Controller Design

The leader is primarily responsible for manipulating the object such that it satisfies the given spatio-temporal task encoded by ϕ. An efficient way to achieve this is by employing Prescribed Performance Control (PPC) [22]. PPC offers a methodology for imposing pre-defined transient and steady-state constraints in the system trajectory. In particular, it confines a tracking error $e(t)$ within predefined regions whose boundaries are defined by time-dependent functions $\pm\gamma(t)$, called performance functions. The mathematical definition of such regions is given by $-\gamma(t) < e(t) < \gamma(t)$. Note that such inequalities naturally encode spatio-temporal constraints, which motivates us to employ the PPC methodology for the accommodation of the given STL task. In particular, one can define a desired reference pose trajectory $x_d(t)$, the associated error

$$e_x = [e_{px}, \dots, e_\psi]^\top = x_o - x_d \tag{16}$$

and exponentially-decaying performance functions $\gamma_x(t) = \text{diag}(\gamma_{px}, \gamma_{py}, \gamma_{pz}, \gamma_\phi, \gamma_\theta, \gamma_\psi)$ and $\gamma_{x_i}(t) = (\gamma_{x_i}^0 - \gamma_{x_i}^\infty)\exp(-lt) + \gamma_{x_i}^\infty$ with $\gamma_{x_i}^0 > |e_{x_i}(0)|$, such that $-\gamma_{x_i}(t) < e_{x_i}(t) < \gamma_{x_i}(t)$ implies the satisfaction of the STL task ϕ. This is accomplished by appropriately tuning the decaying rate constants $l \in \mathbb{R}_+$ and final converging value $\gamma_{x_i}^\infty$. More information can be found in our previous work [17].

For the exposition below, we focus on the scenario involving a single leader, i.e., $N_l = 1$. However, the findings are extendable to scenarios in which multiple leaders cooperate with each other.

Using (14), the leader-follower-object dynamics takes the form,

$$\tilde{M}\dot{v}_o + (\tilde{C} + K_v)v_o + (g_o - Y_o\hat{\gamma}_o) + G_l^\top g_l - J_{o_r}^{-1} K_x \Delta x_e = G_l^\top u_l. \tag{17}$$

The goal now is to design the leader controller u_l so that a desired spatio-temporal task on the object is enforced by achieving the PPC specifications.

Step I: Define the normalised errors $\xi_x \in \mathbb{R}^6$ by,

$$\xi_x = [\xi_{px}, \dots, \xi_\psi]^\top = \gamma_x^{-1}(t) e_x(t) \tag{18}$$

and design the reference velocity as

$$v_r(t) = -c_1 J_{o_r} \gamma_x^{-1}(t) r_x(\xi_x) \varepsilon_x(\xi_x) \tag{19}$$

where c_1 is a positive constant and the signals $\varepsilon_x : (-1,1)^6 \to \mathbb{R}^6$ and $r_x : (-1,1)^6 \to \mathbb{R}^{6\times 6}$ are $\varepsilon_x(\xi_x) = [\varepsilon_{px}, \dots, \varepsilon_\psi]$ and $r_x(\xi_x) = \text{diag}([r_i]_{i\in\{px,\dots,\psi\}})$, with,

$$\varepsilon_{x_i} = \ln\Big(\frac{1+\xi_{x_i}}{1-\xi_{x_i}}\Big),\ r_{x_i} = \frac{2}{1-\xi_{x_i}^2}, i \in \{px, py, pz, \phi, \theta, \psi\}.$$

Step II: Define the velocity error $e_v \in \mathbb{R}^6$ as,

$$e_v = [e_{vx}, \dots, e_{\omega_z}]^\top = v_o - v_r \tag{20}$$

where $v_o = [\dot{p}_o^\top, \omega_o^\top]^\top \equiv [vx, vy, vz, \omega_x, \omega_y, \omega_z]^\top$. Let the velocity performance functions $\gamma_v(t) = \text{diag}(\gamma_{vx}, \gamma_{vy}, \gamma_{vz}, \gamma_{\omega_x}, \gamma_{\omega_y}, \gamma_{\omega_z})$ and $\gamma_v(t) = (\gamma_v^0 - \gamma_v^\infty)\exp(-lt) + \gamma_v^\infty$ with $\gamma_v^0 > |e_v(0)|$. Choose $l \in \mathbb{R}_+$ and γ_v^∞ such that the desired velocity constraints are satisfied if $-\gamma_v(t) < e_v(t) < \gamma_v(t)$ holds.

Step III: Define the normalised errors $\xi_v \in \mathbb{R}^6$ by,

$$\xi_v = [\xi_{vx}, \dots, \xi_{\omega_z}]^\top = \gamma_v^{-1}(t) e_v(t) \tag{21}$$

and design the control law in (17) as

$$u_l(t) = -c_2 J_{o_l}^{-1} \gamma_v^{-1}(t) r_v(\xi_x) \varepsilon_v(\xi_v) \tag{22}$$

where J_{o_l} is the object to leader Jacobian, c_2 is a positive constant and the signals $\varepsilon_v : (-1,1)^6 \to \mathbb{R}^6$ and $r_v : (-1,1)^6 \to \mathbb{R}^{6\times 6}$ are $\varepsilon_v(\xi_v) = [\varepsilon_{vx}, \dots, \varepsilon_{\omega_z}]$ and $r_v(\xi_v) = \text{diag}([r_i]_{i\in\{vx,\dots,\omega_z\}})$, with,

$$\varepsilon_{v_i} = \ln\Big(\frac{1+\xi_{v_i}}{1-\xi_{v_i}}\Big), r_{v_i} = \frac{2}{1-\xi_{v_i}^2}, i \in \{vx, vy, vz, \omega_x, \omega_y, \omega_z\}.$$

Before we demonstrate that the proposed control scheme ensures the containment of trajectories within the designated performance functions, we will state the following assumption.

Assumption 1: The object's pose does not result in a singular $J_{o_r}(x_o(t))$, i.e. $\theta_o(t) \in [-\bar{\theta}, \bar{\theta}]$, for all $t \geq 0$, with $\bar{\theta} \in (0, \frac{\pi}{2})$.

Theorem 2: Consider a leader-follower system rigidly grasping an object with coupled dynamics (8) and subject to spatio-temporal tasks requiring x_o to track a desired trajectory x_d under timing constraints. Then the controller (22) guarantees $-\gamma_x(t) < e_x(t) < \gamma_x(t)$ for all $t \geq 0$, and the boundedness of all closed loop signals.

Proof: Consider first the dynamics of the normalised error $\dot{\xi}_x = \gamma_x^{-1}(\dot{e}_x - \dot{\gamma}_x \xi_x)$, which after using (18), (19) and (20) becomes,

$$\dot{\xi}_x = f_x(\xi_x, t) = \\ -c_1 \|\varepsilon_x r_x \gamma_x^{-1}\| - \varepsilon_x^\top r_x \gamma_x^{-1}(\dot{\gamma}_x \xi_x - J_{o_r}^{-1} \gamma_v \xi_v). \tag{23}$$

Define the open and nonempty set $\Omega_{\xi_x} \subset \mathbb{R}^6$ with $\Omega_{\xi_x} = (-1,1)^6$. We proceed in two steps, first showing that there exists a maximal solution $\xi_x : [t_o, \tau_{\max}) \to \Omega_{\xi_x}$ and then showing that $\tau_{\max} = \infty$. By choosing $\xi_x(t_0)$ as in Step I above, we ensure that $\xi_x(t_0) \in \Omega_{\xi_x}$. Notice also that $f_x(\xi_x, t)$ is continuous in t and locally Lipschitz in ξ_x over Ω_{ξ_h}. Therefore, [23, Theorem 54] yields the existence of a maximal solution $\xi_x : [t_0, \tau_{\max}) \to \Omega_{\xi_x}$. Thus,

$$\xi_x(t) = \frac{e_{x_i}(x_o, t)}{\gamma_{x_i}(t)} \in (-1, 1). \tag{24}$$

$\forall i \in \{px, py, pz, \phi, \theta, \psi\}, t \in [t_0, \tau_{\max})$ from which we conclude $e_{x_i}(t)$ is bounded by $\gamma_{x_i}(t)$. Consider now the positive-definite and radially unbounded function $V_x(\varepsilon_x) = \frac{1}{2}\varepsilon_x^\top \varepsilon_x$. The time derivative of V_x is,

$$\begin{aligned}\dot{V}_x &= \varepsilon_x^\top(\xi_x) r_x(\xi_x)\dot{\xi}_x \\ &\leq -c_1\|\varepsilon_x r_x \gamma_x^{-1}\|^2 - \varepsilon^\top r_x \gamma^{-1}(\dot{\gamma}_x \xi_x - J_{o_r}^{-1}\gamma_v \xi_v)\end{aligned}$$

In the second term above, we have $\xi_x \leq \sqrt{6}$ and $\xi_v \leq \sqrt{6}$, γ_v and $\dot{\gamma}_x$ are bounded for all $t \geq 0$ by construction, and $J_{o_r}^{-1}$ is bounded due to Assumption 1 and due its continuity. All these bounds are also independent of $\tau_{\max}$. Hence $\dot{V}_x$ reduces to

$$\dot{V}_x \leq -c_1\|\varepsilon_x r_x \gamma_x^{-1}\|^2 + \|\varepsilon_x r_x \gamma_x^{-1}\|\bar{B}_x$$

where $\bar{B}_x \geq \|\dot{\gamma}_x \xi_x - J_{o_r}^{-1}\gamma_v \xi_v\|$ and is independent of $\tau_{\max}$. Therefore, we can conclude $\dot{V}_x < 0 \Leftrightarrow \|\varepsilon_x r_x \gamma_x^{-1}\| > \frac{\bar{B}_x}{c_1}$, which, by noting $r_{x_i} > 2$, is equivalent to,

$$\dot{V}_x < 0 \Leftrightarrow \|\varepsilon_x(\xi_x)\| > \frac{\bar{B}_x \max\{\gamma_x(t_0)\}}{c_1}.$$

Therefore, it holds that $\|\varepsilon_x(\xi_x)\| \leq \bar{\varepsilon}_x$, where

$$\bar{\varepsilon}_x = \max\left\{\|\varepsilon_x(\xi_x(t_0))\|, \frac{\bar{B}_x \max\{\gamma_x(t_0)\}}{c_1}\right\}$$

$\forall t \in [t_0, \tau_{\max})$, and taking the inverse logarithm,

$$-1 < \frac{\exp(-\bar{\varepsilon}_x) - 1}{\exp(-\bar{\varepsilon}_x) + 1} \leq \xi_x(t) \leq \frac{\exp(\bar{\varepsilon}_x) - 1}{\exp(\bar{\varepsilon}_x) + 1} < 1.$$

Hence, v_r and consequently $v_o = \gamma_v \xi_v + v_r$ remain bounded for all $t \in [t_0, \tau_{\max})$. We can proceed in a similar manner defining the dynamics $\dot{\xi}_v = f_v(\xi_v(t))$ and constructing the function $V_v = \frac{1}{2}\varepsilon_v^\top \varepsilon_v$. Similar boundedness argument follows for the following terms: (i) the matrix $\tilde{M}$ remains bounded under Assumption 1, (ii) the adaptive update law (13) is stable, (iii) the gravity vectors g_o, g_l and g_f come from the partial derivative of the potential energy of the system and are bounded [24, Property 2.8] (iv) Δx_e is an output from a stable filter and is bounded. And we arrive at similar bounds for ε_v, where $\|\varepsilon_v(\xi_v)\| \leq \bar{\varepsilon}_v$, where

$$\bar{\varepsilon}_v = \max\left\{\|\varepsilon_v(\xi_v(t_0))\|, \frac{\bar{B}_v \max\{\gamma_v(t_0)\}}{c_2 \lambda_{\min}(\tilde{M})}\right\}$$

$\forall t \in [t_0, \tau_{\max})$, where $\lambda_{\min}(\cdot)$ denotes the minimum eigenvalue; by invoking the inverse logarithmic function, we obtain

$$-1 < \frac{\exp(-\bar{\varepsilon}_v) - 1}{\exp(-\bar{\varepsilon}_v) + 1} \leq \xi_v(t) \leq \frac{\exp(\bar{\varepsilon}_v) - 1}{\exp(\bar{\varepsilon}_v) + 1} < 1,$$

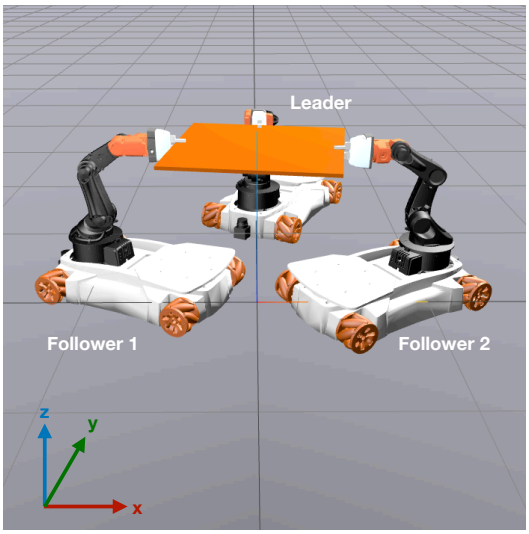

Fig. 2: Setup of 3 YouBots grasping an object.

for all $t \in [t_0, \tau_{\max})$, and hence the boundedness of the proposed control law (22). To complete the proof, we observe that $\xi_x(t)$ and $\xi_v(t)$ are in a compact subset of Ω_x and Ω_v. Therefore, by [23, Prop. C.3.6], we conclude the forward completeness of the solution and $\tau_{\max} = \infty$. ■

Above, we developed a controller for a leader agent aimed at fulfilling the spatio-temporal tasks associated with the object. This controller is not required when a leader agent is substituted by a human operating the object. The strength of the framework developed herein lies in the decoupling of the follower-object system from the leader system. Consequently, the leader can be any entity that possesses knowledge of the tasks imposed on the object being carried.

VI. Simulations

We conduct computer simulations using the realistic environment created by the Drake toolbox [25]. The mobile manipulators under consideration are the KUKA YouBots, which feature an omnidirectional mobile base and a 5-degree-of-freedom manipulator arm equipped with a finger gripper. Our simulation setup includes two follower agents and one leader agent, along with a slab (of mass $m_o = 0.05$[kg]) representing the object, as shown in Figure 2. Let $x_o(t) = [p_o^\top, \eta_o^\top]^\top$ denote the pose of the object's centre of mass, and the initial conditions are $x_o(0) = [0, 0, 0.4, 0, 0, 0]^\top$. The STL formula we impose on the object here is,

$$\begin{aligned}\varphi = &\mathcal{F}_{[0,55]}\Big(\|p_o - [1,1,0.4]^\top\| \leq 3\Big) \wedge \\ &\mathcal{F}_{[55,105]}\Big(\|p_o - [0,1.414,0.4]^\top\| \leq 3\Big) \wedge \\ &\mathcal{F}_{[105,155]}\Big(\|p_o - [-1,1,0.4]^\top\| \leq 3\Big) \wedge \\ &\mathcal{F}_{[155,205]}\Big(\|p_o - [-1.414,0,0.4]^\top\| \leq 3\Big) \wedge \\ &\mathcal{F}_{[205,255]}\Big(\|p_o - [0,0,0.4]^\top\| \leq 3\Big) \wedge \\ &\mathcal{G}_{[255,350]}\Big(\|p_o - [0,0,0.4]^\top\| \leq 3\Big).\end{aligned}$$

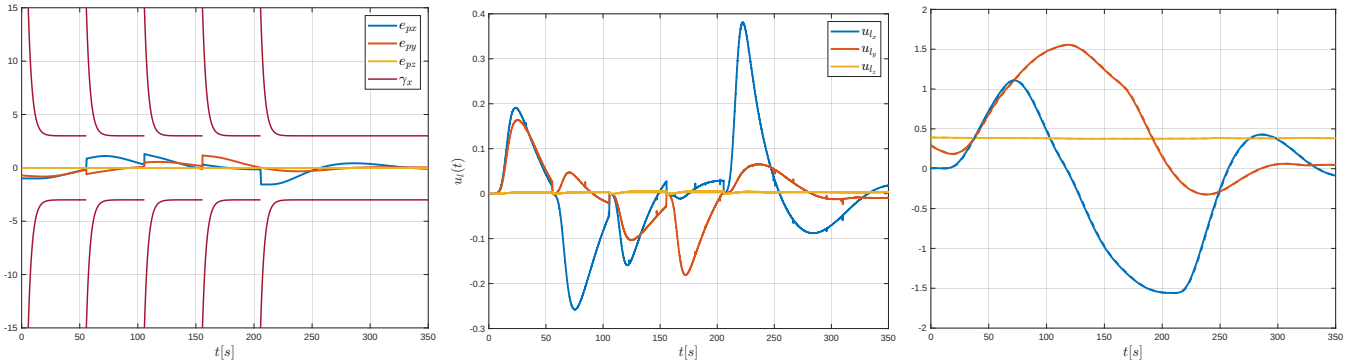

(a) Errors with funnels. (b) Control input of the leader. (c) Evolution of x_o(solid) and x_{o_d}(dotted).

Fig. 3: Results pertaining to a simulation run of the setup in Figure 2.

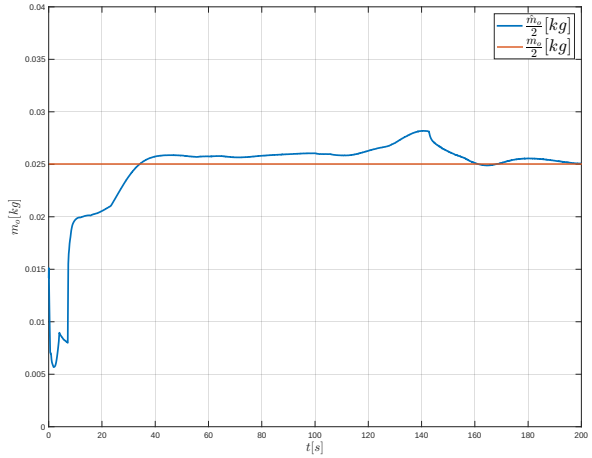

Fig. 4: Estimated mass of the object using (13).

Based on our previous work [17], the STL formula above can be transformed into the following task explanation:

- The desired position p_o of the object should be $[1, 1, 0.4][m]$ at $t_1 = 55$[s], (see Figure 5a),
- Next, the object's desired position should be $[0, 1.414, 0.4][m]$ at $t_2 = 105$[s], (see Figure 5b),
- Next, the object's desired position should be $[-1, 1, 0.4][m]$ at $t_3 = 155$[s], (see Figure 5c),
- Next, the object's desired position should be $[-1.414, 0, 0.4][m]$ at $t_4 = 205$[s], (see Figure 5d),
- And finally, the object should return to the initial conditions at $t_5 = 255$[s] (see Figure 5e) and stay there until $t_6 = 350$[s].

Only the leader is aware of the aforementioned tasks. The error was defined as $e(t) = p_o - p_{o_d}$ where p_{o_d} is the desired position mentioned above. The position and velocity performance functions were chosen as,

$$\gamma(t) = (15 - 3)\exp(-0.3(t - t^*)) + 3$$

where $t^* \in \{0, 55, 105, 155, 205\}$[s]. The results are presented in Figure 3, and snapshots of the simulation environment are depicted in Figure 5. In Figure 3a, we observe the five funnels that enforce the desired transient constraints on the object's position error. It is noted that the errors are contained within the funnels. Figure 3b illustrates the leader control input (22), while Figure 3c displays the object's position as a solid line and the exponential moving average as a dotted line. As can be seen, x_{o_d} closely follows the original position x_o. In Figure 4, the follower agents implement the adaptive law (13) to estimate the mass of the object. As can be seen, the mass of the object converges to 0.025[kg] which is half of the original mass. This is due to the fact that there are two follower agents that share the load of the object equally and, hence, arrive at this estimate.

VII. Conclusions

In this work, we presented a decentralized control algorithm for addressing the cooperative manipulation problem within the context of a leader-follower system framework. We demonstrated the decoupling of the primary objective, which involves fulfilling spatio-temporal tasks, from the secondary objective of carrying the object. The primary task is executed by the leader agent, equipped with a PPC controller, whereas the secondary task is undertaken by the follower agents, whose sole purpose is to help compensate the object's gravitational force. Furthermore, we provided experimental validation of the proposed framework through simulations involving KUKA YouBot robots.

References

[1] T. Hsia, "Adaptive control of robot manipulators - a review," in *Proceedings. 1986 IEEE International Conference on Robotics and Automation*, vol. 3, 1986, pp. 183–189.

[2] P. Tomei, "Adaptive pd controller for robot manipulators," *IEEE Transactions on Robotics and Automation*, vol. 7, no. 4, pp. 565–570, 1991.

[3] R. Kelly, R. Carelli, M. Amestegui, and R. Ortega, "On adaptive impedance control of robot manipulators," in *Proceedings, 1989 International Conference on Robotics and Automation*, 1989, pp. 572–577 vol.1.

[4] T. Yang, N. Sun, Y. Fang, X. Xin, and H. Chen, "New adaptive control methods for n-link robot manipulators with online gravity compensation: Design and experiments," *IEEE Transactions on Industrial Electronics*, vol. 69, no. 1, pp. 539–548, 2022.

[5] J. Fujishiro, Y. Fukui, and T. Wada, "Finite-time pd control of robot manipulators with adaptive gravity compensation," in *2016 IEEE Conference on Control Applications (CCA)*, 2016, pp. 898–904.

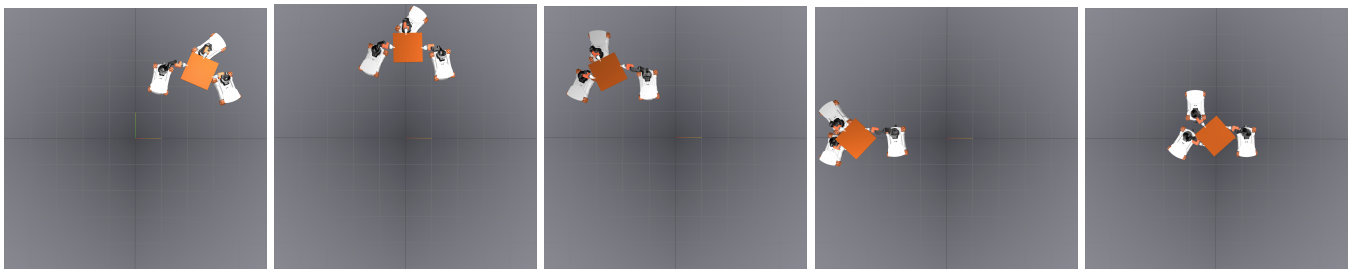

(a) At $t = 55s$ (b) At $t = 105s$ (c) At $t = 155s$ (d) At $t = 205s$ (e) At $t = 255s$

Fig. 5: Snapshots of the simulation environment at various timestamps.

[6] A. Dietrich, C. Ott, and A. Albu-Schäffer, "Multi-objective compliance control of redundant manipulators: Hierarchy, control, and stability," in *2013 IEEE/RSJ International Conference on Intelligent Robots and Systems*, 2013, pp. 3043–3050.

[7] R. Nebbia Colomba, R. Laha, L. F. Figueredo, and S. Haddadin, "Adaptive admittance control for cooperative manipulation using dual quaternion representation and logarithmic mapping," in *2022 IEEE 61st Conference on Decision and Control (CDC)*, 2022, pp. 107–144.

[8] A. Albu-Schaffer, C. Ott, U. Frese, and G. Hirzinger, "Cartesian impedance control of redundant robots: recent results with the dlr-light-weight-arms," in *2003 IEEE International Conference on Robotics and Automation (Cat. No.03CH37422)*, vol. 3, 2003, pp. 3704–3709 vol.3.

[9] C. Jiao, L. Yu, X. Su, Y. Wen, and X. Dai, "Adaptive hybrid impedance control for dual-arm cooperative manipulation with object uncertainties," *Automatica*, vol. 140, p. 110232, 2022. [Online]. Available: https://www.sciencedirect.com/science/article/pii/S0005109822000772

[10] M. Van Damme, P. Beyl, B. Vanderborght, V. Grosu, R. Van Ham, I. Vanderniepen, A. Matthys, and D. Lefeber, "Estimating robot end-effector force from noisy actuator torque measurements," in *2011 IEEE International Conference on Robotics and Automation*, 2011, pp. 1108–1113.

[11] W.-H. Chen, D. Ballance, P. Gawthrop, and J. O'Reilly, "A nonlinear disturbance observer for robotic manipulators," *IEEE Transactions on Industrial Electronics*, vol. 47, no. 4, pp. 932–938, 2000.

[12] W. Dixon, I. Walker, D. Dawson, and J. Hartranft, "Fault detection for robot manipulators with parametric uncertainty: a prediction-error-based approach," *IEEE Transactions on Robotics and Automation*, vol. 16, no. 6, pp. 689–699, 2000.

[13] A. De Luca and R. Mattone, "Actuator failure detection and isolation using generalized momenta," in *2003 IEEE International Conference on Robotics and Automation (Cat. No.03CH37422)*, vol. 1, 2003, pp. 634–639 vol.1.

[14] A. Tsiamis, C. K. Verginis, C. P. Bechlioulis, and K. J. Kyriakopoulos, "Cooperative manipulation exploiting only implicit communication," in *2015 IEEE/RSJ International Conference on Intelligent Robots and Systems (IROS)*, 2015, pp. 864–869.

[15] M. Logothetis, C. P. Bechlioulis, and K. J. Kyriakopoulos, "Decentralized impedance control of mobile robotic manipulators for collaborative object handling with a human operator," in *2021 29th Mediterranean Conference on Control and Automation (MED)*, 2021, pp. 741–746.

[16] M. Zribi, S. Ahmad, and S. Luo, "Adaptive control of redundant multiple robots in cooperative motion," *Journal of Intelligent and Robotic Systems*, vol. 17, pp. 169–194, 1996.

[17] M. Sewlia, C. K. Verginis, and D. V. Dimarogonas, "Cooperative object manipulation under signal temporal logic tasks and uncertain dynamics," *IEEE Robotics and Automation Letters*, vol. 7, no. 4, pp. 11 561–11 568, 2022.

[18] O. Khatib, "A unified approach for motion and force control of robot manipulators: The operational space formulation," *IEEE Journal on Robotics and Automation*, vol. 3, no. 1, pp. 43–53, 1987.

[19] O. Maler and D. Nickovic, "Monitoring Temporal Properties of Continuous Signals," in *Formal Techniques, Modelling and Analysis of Timed and Fault-Tolerant Systems*, ser. Lecture Notes in Computer Science, Y. Lakhnech and S. Yovine, Eds. Berlin, Heidelberg: Springer, 2004, pp. 152–166.

[20] J. P. LaSalle, "Stability theory and invariance principles," in *Dynamical systems*. Elsevier, 1976, pp. 211–222.

[21] O. Khatib, "Motion/force redundancy of manipulators," in *Proceedings of Japan-USA Symposium on Flexible Automation*, vol. 1, 1990, pp. 337–342.

[22] C. P. Bechlioulis and G. A. Rovithakis, "A low-complexity global approximation-free control scheme with prescribed performance for unknown pure feedback systems," *Automatica*, vol. 50, no. 4, pp. 1217–1226, 2014. [Online]. Available: https://www.sciencedirect.com/science/article/pii/S0005109814000582

[23] E. D. Sontag, *Mathematical Control Theory: Deterministic Finite Dimensional Systems*. Springer-Verlag New York, 1998, oCLC: 1165444109.

[24] C. Ott, *Cartesian impedance control of redundant and flexible-joint robots*. Springer, 2008.

[25] R. Tedrake and the Drake Development Team, "Drake: Model-based design and verification for robotics," 2019. [Online]. Available: https://drake.mit.edu